PD1-based DNA vaccine amplifies HIV-1 GAG-specific CD8+ T cells in mice

Jingying Zhou,[1] Allen K.L. Cheung,[1] Zhiwu Tan,[1] Haibo Wang,[1] Wenbo Yu,[1] Yanhua Du,[1] Yuanxi Kang,[1] Xiaofan Lu,[1] Li Liu,[1] Kwok-Yung Yuen,[1,2] and Zhiwei Chen[1,2]

[1]AIDS Institute and Department of Microbiology and [2]Research Center for Infection and Immunity, Li Ka Shing Faculty of Medicine,
The University of Hong Kong, Hong Kong, China.

Viral vector–based vaccines that induce protective CD8+ T cell immunity can prevent or control pathogenic SIV infections, but issues of preexisting immunity and safety have impeded their implementation in HIV-1. Here, we report the development of what we believe to be a novel antigen-targeting DNA vaccine strategy that exploits the binding of programmed death-1 (PD1) to its ligands expressed on dendritic cells (DCs) by fusing soluble PD1 with HIV-1 GAG p24 antigen. As compared with non–DC-targeting vaccines, intramuscular immunization via electroporation (EP) of the fusion DNA in mice elicited consistently high frequencies of GAG-specific, broadly reactive, polyfunctional, long-lived, and cytotoxic CD8+ T cells and robust anti-GAG antibody titers. Vaccination conferred remarkable protection against mucosal challenge with vaccinia GAG viruses. Soluble PD1–based vaccination potentiated CD8+ T cell responses by enhancing antigen binding and uptake in DCs and activation in the draining lymph node. It also increased IL-12–producing DCs and engaged antigen cross-presentation when compared with anti-DEC205 antibody-mediated DC targeting. The high frequency of durable and protective GAG-specific CD8+ T cell immunity induced by soluble PD1–based vaccination suggests that PD1-based DNA vaccines could potentially be used against HIV-1 and other pathogens.

Introduction

HIV-1 is one of the most devastating infectious agents existing worldwide for the past 30 years. Viral latency, high rates of mutation during viral replication, and emergence of drug-resistant strains are posing problems for highly active antiretroviral therapy (HAART) despite the ongoing development of newer drugs (1–3). An effective vaccine against HIV-1, therefore, remains a top priority in the fight against this pandemic virus. The induction of a high frequency of protective T cell immunity is a prerequisite for the successful control by a vaccine of intracellular pathogenic infections, and this has been well documented in the case of HIV-1 (4–7). Viral vector–based vaccines that induce such immunity can prevent or control pathogenic SIV infections, but issues of preexisting immunity and safety surround their implementation (8–10). DNA vaccines have shown a certain effectiveness, with a low level of toxicity in animal and human trials (11). However, conventional DNA vaccines with only the encoded antigen failed to mount a high frequency of effective CD8+ T cell immunity, even when delivered by in vivo electroporation (EP) (12, 13). Therefore, targeting DNA vaccines to cells with ample antigen-presenting capacity, such as dendritic cells (DCs), has been the focus in recent years. Significant progress has been made, including DNA vaccines delivered by EP, in targeting antigens to DCs via various surface proteins expressed by DCs in order to augment antibody and T cell responses. However, targeting via anti-DEC205 antibody and soluble (s)CTLA-4 (cytotoxic T lymphocyte antigen 4) resulted in only a low frequency of antigen-specific CD8+ T cell immunity (14–18). To date, it remains unclear which DC receptor targets would intensify antigen-specific CD8+ T cell immunity.

Along these lines, targeting vaccine antigens to DCs via the native ligands of programmed death-1 (PD1/CD279), namely PD-L1/CD274 and PD-L2/CD273, in order to enhance immunogenicity has not been studied before. PD-L1 is constitutively expressed on T cells, B cells, macrophages, and DCs, whereas PD-L2 is found on DCs and activated monocytes and macrophages (19, 20). The essential role of the PD1/PD-L pathway in modulating immunity against chronic viral infections (e.g., HIV, HCV) and cancer has been well established (21–24). Upregulated expression of PD1 is associated with the exhaustion of T and B cell functions. Thus, blockade of the PD1/PD-L pathway using anti-PD1 antibody or a soluble form of PD1 (sPD1) that contains only the extracellular domain rescues exhausted T cell responses and enhances antiviral and antitumor immunity (25–27). The role of sPD1 in modulating adaptive immune responses in the context of vaccination remains largely unknown. Since the level and distribution of PD-L expression on DCs may be different from other DC receptors (e.g., DEC205), it is of interest to determine whether an sPD1-based vaccine would elicit adaptive immunity with unique characteristics. We therefore hypothesize that an sPD1-based vaccine may improve adaptive T cell immunity by targeting vaccine antigens to DCs via PD-L1/L2 in vivo. To test this hypothesis, we chose HIV-1 GAG p24 as a test antigen because it has been commonly used in other DC-targeting strategies as a model immunogen (15, 28). Moreover, mounting evidence supports an essential role of potent and durable GAG-specific CD8+ T cell immunity in containing SIV/HIV infections (9, 29, 30), but conventional HIV-1 vaccination has been disappointing in terms of inducing these responses preclinically and clinically (11, 31–34). In this study, we report what we believe to be a novel sPD1-based DNA/EP vaccination strategy that is uniquely immunogenic in its ability to induce high frequencies of durable, polyfunctional, cytotoxic, and protective GAG-specific CD8+ T cells. Moreover, we uncovered possible mechanisms underlying the greatly enhanced immunogenicity of this strategy.
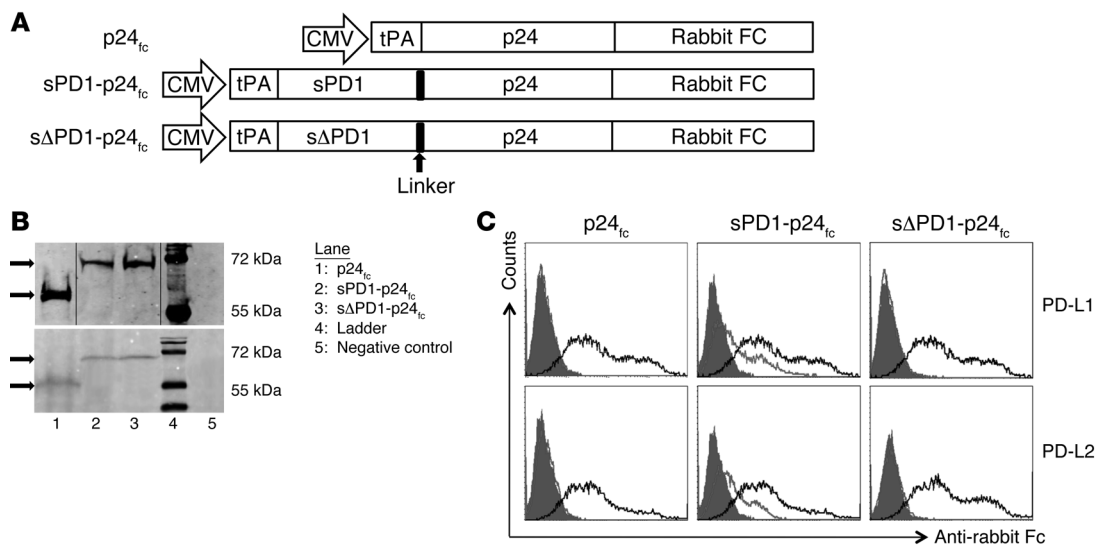
Figure 1
Expression and binding characteristics of DNA vaccine constructs. (**A**) Schematic representation of constructs encompassing the soluble form of PD1 (sPD1) or with 2 amino acid deletions essential for binding with PD-L1/L2 (sΔPD1), p24, and rabbit Fc under the CMV promoter, denoted as sPD1-p24$_{fc}$, sΔPD1-p24$_{fc}$, and p24$_{fc}$, respectively. All constructs contain a tissue plasminogen activator (tPA) signal sequence. Rabbit Fc was used as a tag for purification and detection purposes. (**B**) Expression of fusion constructs as purified recombinant proteins examined by Western blot. Upper and lower blots show proteins detected by anti-HIV GAG or anti-rabbit Fc antibody, respectively. Smaller-sized bands (lower panel arrows) represent p24$_{fc}$, while the larger-sized bands (upper panel arrows) represent sPD1-p24$_{fc}$ or sΔPD1-p24$_{fc}$. Lanes are identified by the legend and numbers in kDa indicate marker sizes. (**C**) 293T cells were transiently transfected with PD-L1 or PD-L2 expression vectors, and the binding profiles of recombinant proteins were examined by flow cytometry using anti-rabbit Fc-FITC detection antibody (gray line). Controls included transfected 293T cells stained with anti-rabbit Fc-FITC antibody (negative, shaded line) or anti-mouse PD-L1 or L2 antibodies (positive, solid line).

Results

Generation of sPD1-based fusion DNA vaccines. Three DNA vaccines: p24$_{fc}$, sPD1-p24$_{fc}$, and sΔPD1-p24$_{fc}$, consisting of various combinations of sPD1 or sΔPD1, HIV-1 GAG p24 (p24), and rabbit Fc (fc) were designed and generated to test our working hypothesis (Figure 1A). The rabbit Fc helps protein detection and purification but does not contain its receptor-binding domain (FcR). sΔPD1 does not bind PD1 ligands due to 2 amino acid deletions in the IgV region (35, 36). The expression of fusion proteins encoded by these DNA vaccines was detected by Western blot analysis using either anti-GAG p24 (Figure 1B, top) or anti-rabbit Fc antibody (Figure 1B, bottom). To determine whether recombinant proteins expressed from these DNA vaccines could interact with PD1 ligands, we purified corresponding soluble proteins for binding to 293T cells transiently expressing PD-L1 or PD-L2 and used a detection antibody against rabbit Fc for analysis with flow cytometry (Figure 1C). Indeed, PD-L1 and PD-L2 interacted only with recombinant sPD1-p24$_{fc}$ protein, but not with sΔPD1-p24$_{fc}$ or p24$_{fc}$ proteins.

sPD1-p24$_{fc}$/EP DNA vaccination enhances p24-specific CD8$^+$ T cell immunity and antibody responses in vivo. The 3 DNA vaccines were subsequently evaluated in vivo for their immunogenicity. Since intramuscular EP (referred to hereafter as i.m./EP) improves the immunogenicity of DNA vaccines by enhancing antigen expression and recruiting DCs as previously described (16, 37, 38), we performed sPD1-p24$_{fc}$/EP vaccination in BALB/c mice with an initial dose of 20 μg DNA per shot. We monitored the degree of immune responses 2 weeks after each of the 3 vaccinations (Figure 2A) (31). Compared with non–DC-targeting p24$_{fc}$/EP and sΔPD1-p24$_{fc}$/EP,

we found that 3 vaccinations with sPD1-p24$_{fc}$/EP were essential for eliciting stronger p24-specific T cell responses, with increases in splenocytes (greater than 2-fold) against the H2-K^d–restricted CD8 epitope GAG A-I (approximately 900 spot-forming units [SFUs] per 10^6 cells; Figure 2B) as well as IgG1 (Th2; ~8-fold) and IgG2a (Th1; ~4-fold) antibody responses (Figure 2C) detected by IFN-γ$^+$ ELISPOT and ELISA, respectively. In particular, p24-specific CD8$^+$ T cell responses were consistently more than 10-fold higher than those of CD4$^+$ T cells among all animals tested (Figure 2B). We therefore proceeded with this standard immunization schedule throughout our studies. Critically, since the persistence of induced memory immunity over a long period is important to assess the efficacy of a vaccine, we also determined whether the enhanced p24-specific CD8$^+$ T cell immunity and antibody responses were long lived. Groups of mice were studied 7.5 months after the third immunization. Compared with what was observed 2 weeks after the last vaccination (Figure 2, B and C), only the sPD1-p24$_{fc}$/EP vaccination maintained long-lived p24-specific memory CD8$^+$ T cells (~2-fold decrease; Figure 2D), minimal p24-specific memory CD4$^+$ T cells (less than a 5-fold decrease; Figure 2E), and enhanced IgG1 and IgG2a antibody responses (~2-fold increase; Figure 2F).

Dose-dependent enhancement of broadly reactive p24-specific CD8$^+$ T cell immunity and antibody responses by sPD1-p24$_{fc}$/EP vaccination. To determine the dose effect of sPD1-p24$_{fc}$/EP vaccination, we performed immunization using a 100-μg dose of DNA following the same immunization schedule (Figure 2A) (31). Indeed, compared with the 20-μg dose, we found a further 2-fold increase in both CD8$^+$ and CD4$^+$ T cell responses (Figure 3, A and B), as well as a greater than 10-fold increase in IgG1 and IgG2a antibody
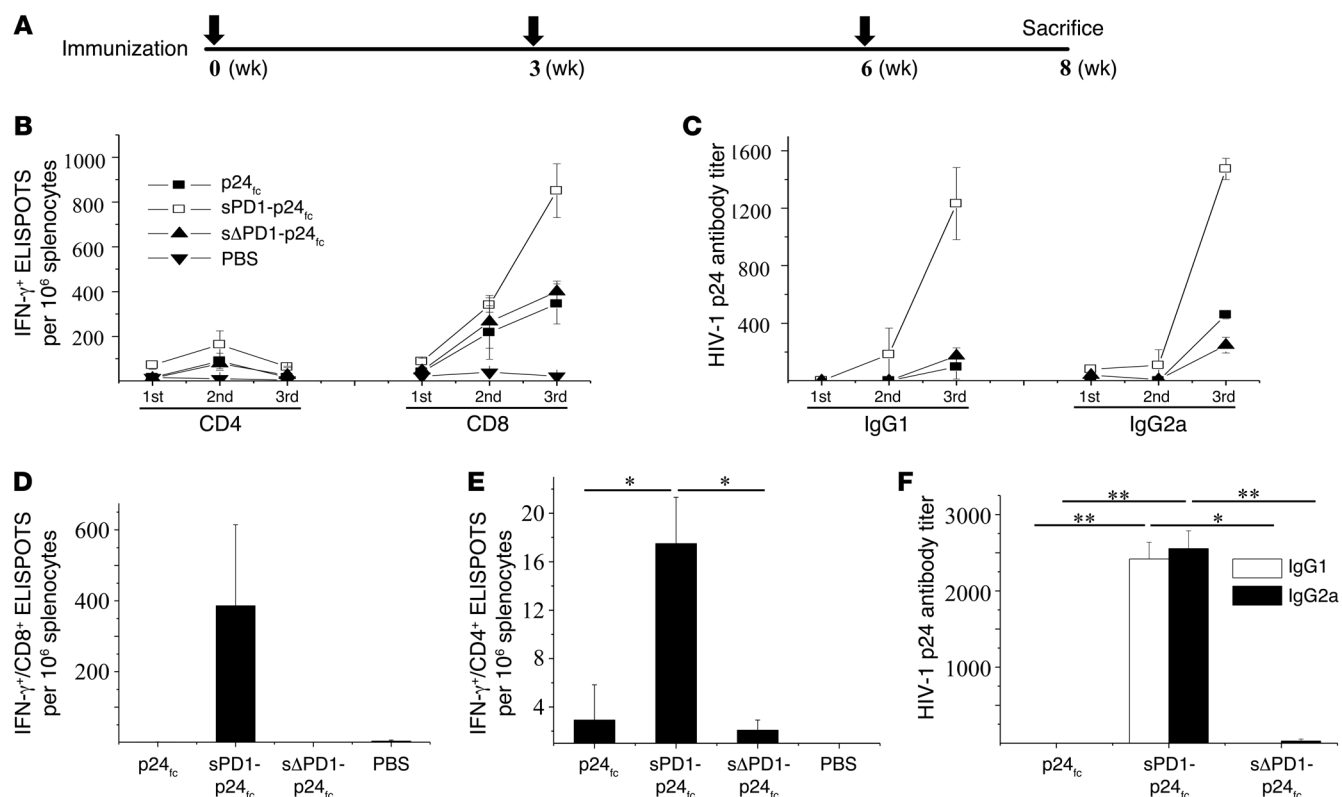
Figure 2
Induction of enhanced and long-lasting p24-specific immune responses by sPD1-p24$_{fc}$ vaccination in optimized conditions. (**A**) DNA vaccine immunization schedule for BALB/c mice. Mice were immunized at weeks 0, 3, and 6. For assessing overall immune response, mice were sacrificed 2 weeks after the last immunization to collect spleen and blood for analysis of cellular and humoral immune responses. (**B**) BALB/c mice were immunized with sPD1-p24$_{fc}$, sΔPD1-p24$_{fc}$, and p24$_{fc}$ at a dose of 20 μg DNA delivered via i.m./EP. Mice that received PBS only served as negative controls. Two weeks after each vaccination, ELISPOT assays for CD8+ T cells and CD4+ T cells were performed to test the ability of T cells to produce IFN-γ in specific response to HIV-1 GAG p24 epitopes GAG A-I (CD8) and GAG 26 (CD4), respectively, as well as to (**C**) IgG1 and IgG2a antibodies specific to HIV-1 p24 in sera detected by ELISA. To determine long-lived immunity, mice were rested for 7.5 months following the immunization regimen before being sacrificed. ELISPOT assays were performed for (**D**) CD8+ T cells and (**E**) CD4+ T cells to test their ability to produce IFN-γ in specific response to HIV-1 GAG p24 epitopes GAG A-I and GAG 26, respectively. (**F**) Specific IgG1 and IgG2a antibodies against HIV-1 GAG p24 detected by ELISA. Data show the means with standard error from 3 independent immunization experiments with 3 mice per group. *$P < 0.05$; **$P < 0.01$.

responses in immunized BALB/c mice 2 weeks after the last vaccination (Figure 3C, left), suggesting a dose-dependent effect. Since T cell immune response is important in the elimination of HIV-1–infected cells, we further tested the epitope specificity of p24-specific T cells. In this case, 3 nonoverlapping peptide pools spanning the entire p24 protein were used as stimuli, and 800–1,000 ELISPOTs per 10^6 splenocytes were detected with each of these pools (Figure 3D, left), indicating substantial breadth of the elicited T cell response in recognizing p24 antigen. Furthermore, we were able to reproduce these results in C57BL/6 mice, showing consistently greater T cell and antibody responses induced by sPD1-p24$_{fc}$/EP vaccination. The significantly enhanced antibody response was skewed toward a Th2 response in C57BL/6 mice, as indicated by a relatively higher IgG1 reactivity than Th1-related IgG2c antibody reactivity (Figure 3C, right; $P < 0.05$). Moreover, close to 1,000 ELISPOTs per 10^6 splenocytes were detected with p24 pool 3, while the variable levels of responses to p24 pools 1 and 2 were probably due to the genetic differences between BALB/c and C57BL/6 mice (e.g., H2-K^d versus H2-K^b) (Figure 3D). Of critical note, more than 13% and 22% of CD8+ T cells in the spleen

were positive for H2-K^d-GAG A-I tetramer binding in the 20-μg and 100-μg sPD1-p24$_{fc}$ dose groups of BALB/c mice, respectively, which were substantially higher percentages than those in the sΔPD1-p24$_{fc}$ or p24$_{fc}$ groups (Figure 4, A and B) (39). In addition, we evaluated the long-term memory CD8+ T cell responses isolated from BALB/c mice 7.5 months after their final 100-μg dose of DNA vaccine. Statistically significant CD8+ T cell ELISPOT responses were detected only in sPD1-p24$_{fc}$/EP–immunized mice (Figure 4C; $P < 0.01$). Importantly, a CFSE proliferation assay of CD8+ T cell response to p24 antigen was also performed to confirm the long-term memory responses. Memory CD8+ T cell proliferation was detected only in sPD1-p24$_{fc}$ mice (Figure 4D). Taken together, sPD1-p24$_{fc}$/EP DNA vaccination elicited, in a dose-dependent manner, robust CD8+ T cell immunity with extended epitopic breadth of p24 specificity, enhanced anti-p24 antibody, and long-term memory responses.

Amplification of polyfunctional and cytotoxic p24-specific CD8+ T cell immunity by sPD1-p24$_{fc}$/EP vaccination. Given the importance of polyfunctional CD8+ T cell response in controlling SIV/HIV-1 infection (9, 40), we measured the ability of p24-specific T cell
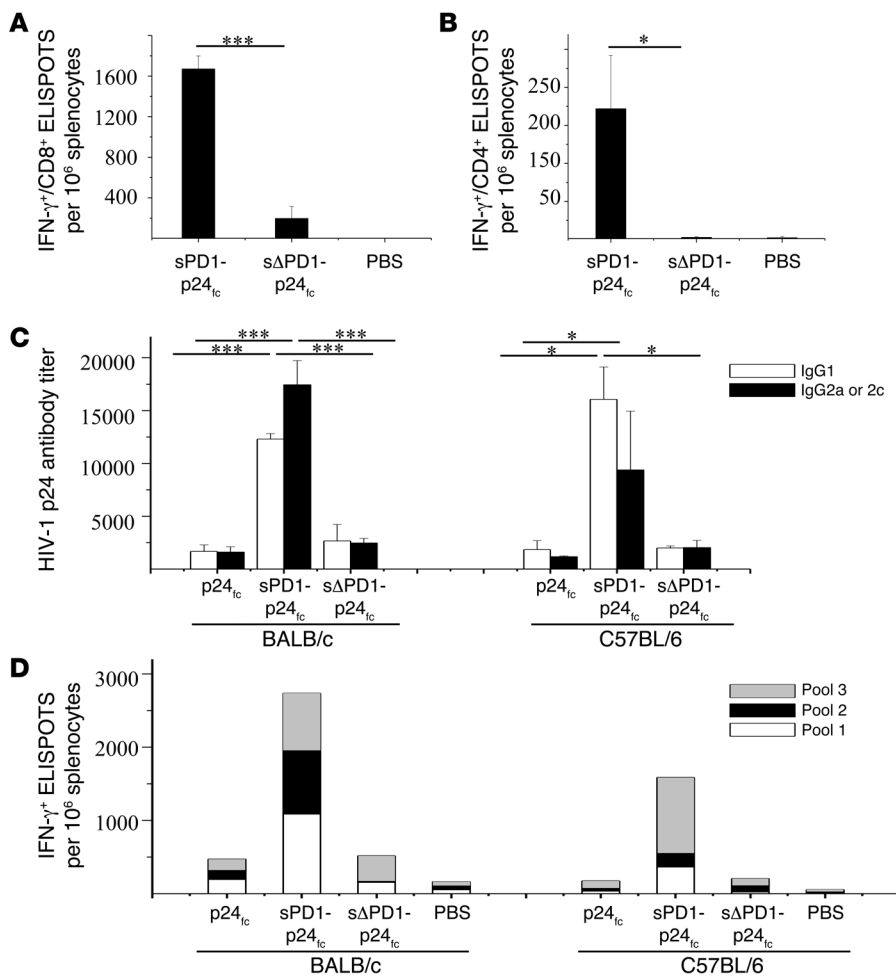
Figure 3
Comparison of sPD1-p24$_{fc}$ elicited antigen-specific immunity in 2 mice models. BALB/c and C57BL/6 mice were vaccinated with sPD1-p24$_{fc}$, sΔPD1-p24$_{fc}$, and p24$_{fc}$ at a dose of 100 μg DNA i.m/EP according to the immunization schedule. (**A**) IFN-γ–producing CD8$^+$ and (**B**) CD4$^+$ cells were measured by ELISPOT assay in BALB/c splenocytes stimulated using the specific peptides GAG A-I and GAG 26, respectively. (**C**) Specific antibodies against HIV-1 GAG p24 detected by ELISA. IgG1 (Th2) was tested in both strains of mice, while IgG2a was detected in BALB/c mice and IgG2c was detected in C57BL/6 mice. (**D**) IFN-γ–secreting cells from splenocytes isolated from BALB/c or C57BL/6 mice in response to stimulation using 3 different nonoverlapping peptide pools derived from 59 peptides spanning the entire HIV-1 GAG p24 region as detected by ELISPOT. Data show the means with standard error from 3 independent immunization experiments with 3 mice per group. *P < 0.05; ***P < 0.001.

populations from immunized mice to secrete IFN-γ, TNF-α, and IL-2 in response to p24 peptide pool stimulation. Our gating strategy of intracellular cytokine flow cytometric analysis is depicted in Figure 5A; this strategy allowed us to separate CD8$^+$ T or CD4$^+$ T cells into subsets based on their ability to produce one or more cytokines (IFN-γ, TNF-α, and IL-2). Compared with sΔPD1-p24$_{fc}$/EP, the sPD1-p24$_{fc}$/EP vaccination elicited substantially higher frequencies of p24-specific IFN-γ$^+$CD8$^+$ T cells, with up to 47.1% of total splenic CD8$^+$ T cells (Figure 5A) producing either IFN-γ alone (21.0%), dual IFN-γ/TNF-α (22.3%), or triple IFN-γ/TNF-α/IL-2 (4.7%) (Figure 5B). The frequencies of p24-specific CD4$^+$ T cells producing IFN-γ alone (2.9%), IFN-γ/TNF-α (3.7%), or IFN-γ/TNF-α/IL-2 (0.9%) were elevated as well with the sPD1-p24$_{fc}$/EP vaccination (Figure 5C). Interestingly, the proportional order of effector CD8$^+$ and CD4$^+$ T cell subpopulations in response to p24 stimulation was similar, with IFN-γ$^+$/TNF-α$^+$ being greater than IFN-γ$^+$, which in turn was greater than IFN-γ$^+$/TNF-α$^+$/IL-2$^+$. The high frequencies of effector cells secreting IFN-γ/TNF-α (CD8$^+$: 44.8%; CD4$^+$: 39.5%), IFN-γ (CD8$^+$: 42.2%; CD4$^+$: 30.4%), and IFN-γ/TNF-α/IL-2 (CD8$^+$: 9.4%; CD4$^+$: 9.7%) among the total p24-specific CD8$^+$ and CD4$^+$ T cell populations are indicative of enhanced vaccine potency induced by sPD1-p24$_{fc}$/EP vaccination (Figure 5D).

Since cytotoxic T cell quality is essential for the elimination of infected cells, we used the mouse mesothelioma cell line AB1 transduced to express HIV-1 GAG (41). Forty-three percent of the

AB1-HIV-1-GAG cells readily expressed HIV-1 p24 (Supplemental Figure 1A; supplemental material available online with this article; doi:10.1172/JCI64704DS1), and these cells were used as target cells for the cytotoxicity assay. Since total splenocytes isolated from sPD1-p24$_{fc}$/EP–immunized mice showed stronger target cell killing effects (Supplemental Figure 1B), we further examined the effectiveness of purified CD8$^+$ and CD4$^+$ T cells from splenocytes using the same assay. As shown in Figure 5E, a high percentage of dead target cells was detected after coculture with CD8$^+$ T cells from sPD1-p24$_{fc}$/EP–immunized mice, even at an effector/target cell ratio (E/T) of 0.1:1, compared with the p24$_{fc}$/EP control group. To our surprise, purified CD4$^+$ T cells after sPD1-p24$_{fc}$/EP vaccination also showed cytotoxic function starting from a 1:1 ratio (Figure 5F), suggesting an extended effect of the sPD1-p24$_{fc}$/EP vaccination that could be overshadowed by the induction of a robust level of p24-specific polyfunctional and cytotoxic CD8$^+$ T cell immunity.

Efficacy of p24-specific T cell immunity. To investigate whether cellular immunity elicited by sPD1-p24$_{fc}$/EP leads to protection, groups of BALB/c mice were first challenged intranasally with 4 × 10^7 PFUs of VTT$_{gagpol}$ (a modified vaccinia virus Tian Tan strain that expresses HIV-1 *gagpol*) 3 weeks after the last vaccination with sPD1-p24$_{fc}$/EP or controls at a dose of 20 μg. Three days later, viral titers in the lungs were quantified using a plaque-forming assay as we previously described (42). Compared with p24$_{fc}$/EP and sΔPD1-p24$_{fc}$/EP groups, there were dramatically reduced viral titers detected in
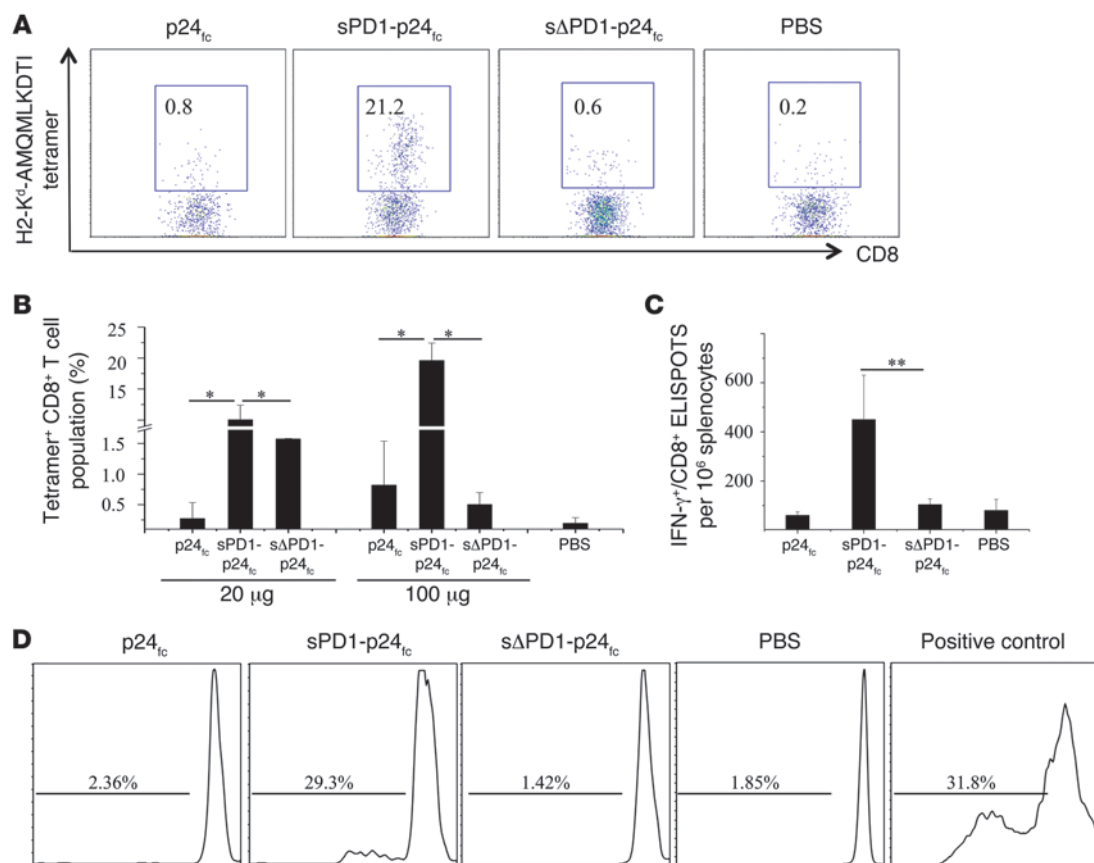
Figure 4

Increased dose of DNA vaccine further enhanced p24-specific tetramer-positive and long-term memory CD8+ T cell responses. sPD1-p24$_{fc}$, sΔPD1-p24$_{fc}$, and p24$_{fc}$ were administered to BALB/c mice at a dose of 100 μg DNA delivered by i.m./EP. (**A**) HIV-1 p24-specific H2-K^d-AMQMLKD-TI-PE tetramer staining of CD8+ T cell populations 2 weeks after the final immunization is shown in flow cytometric plots of 1 representative experiment, or (**B**) in data represented as a column graph of immunization with 2 doses of 20 μg and 100 μg DNA. PBS represents the negative control. (**C**) Thirty weeks after the final i.m./EP vaccination at a dose of 100 μg DNA, IFN-γ–producing CD8+ T cells were measured by ELISPOT assay in splenocytes stimulated using specific GAG A-I epitope. (**D**) Splenocytes labeled with CFSE and stimulated with purified CD11c+ BM-DCs plus p24 peptide pools and anti-CD28 for 5 days. Addition of anti-CD3 antibody served as a positive control. CFSE signals on CD8+ T cell populations were detected by flow cytometry. Data show the SEM from 3 independent immunization experiments with 3 mice per group. *$P < 0.05$; **$P < 0.01$.

mice vaccinated with sPD1-p24$_{fc}$/EP ($P < 0.005$ and $P < 0.01$, respectively) (Figure 6A). VTT$_{gagpol}$, however, is considered an attenuated nonvirulent virus in mice, and the protective effect may be different with pathogenic infection. For this reason, we subsequently generated a virulent vaccinia Western Reserve strain expressing HIV-1 *gagpol* (WR$_{gagpol}$) to challenge mice immunized with a 100-μg DNA vaccine. With an intranasal dose of 2×10^6 PFUs of WR$_{gagpol}$, mice immunized with the placebo, sΔPD1-p24$_{fc}$/EP, or p24$_{fc}$/EP showed greater than 25% body weight loss within 8 days. This contrasts with the mice immunized with sPD1-p24$_{fc}$/EP that showed less than 7% body weight loss (Figure 6B), with a corresponding significant reduction in virus titers in the lungs of this group of mice compared with controls (Figure 6C; $P < 0.01$). Since there was no antivaccinia immunity involved, our data indicate that p24-specific T cell immunity induced by sPD1-p24$_{fc}$/EP provided substantial protection against mucosal challenge in 2 mouse model systems.

Factors contributing to the enhanced immunogenicity of sPD1-p24$_{fc}$/ EP vaccination. To investigate the underlying mechanism of sPD1-p24$_{fc}$/EP vaccination, we compared 4 groups of animals for DNA

vaccination: (a) with EP; (b) no EP; (c) EP/no fusion (i.e., individual sPD1$_{fc}$ and/or p24$_{fc}$ DNA constructs administered simultaneously with EP at the same or different injection sites); and (d) EP/no Fc (sPD1-p24 without the rabbit Fc tag). The latter 3 groups were included to determine the role of EP, protein fusion, and rabbit Fc, respectively, in the induction of enhanced antigen-specific T and B cell immunity. Since CD8+ T cell immune response was low in the "no-EP" animals (data not shown), we used a high dose (100 μg) of sPD1-p24$_{fc}$ DNA for this comparison, whereas a suboptimal 20-μg dose was used for the other 3 groups. Several findings were made in comparison with group 1, which received the sPD1-p24$_{fc}$/EP vaccination. First, the no-EP group elicited 7-fold less IFN-γ+CD8+ T cell ELISPOTs (Supplemental Figure 2A) and 13-fold less IgG2a (Th1) responses, despite a 5-fold increase in vaccine dose (Supplemental Figure 2D), whereas comparable levels of IFN-γ+CD4+ T cell ELISPOTs and IgG1 (Th2) antibody responses were found (Supplemental Figure 2, B and C). Second, the EP/no-fusion group elicited noticeably less T cell (IFN-γ+CD8+ or IFN-γ+CD4+) and IgG2a antibody responses than group 1, with comparable levels
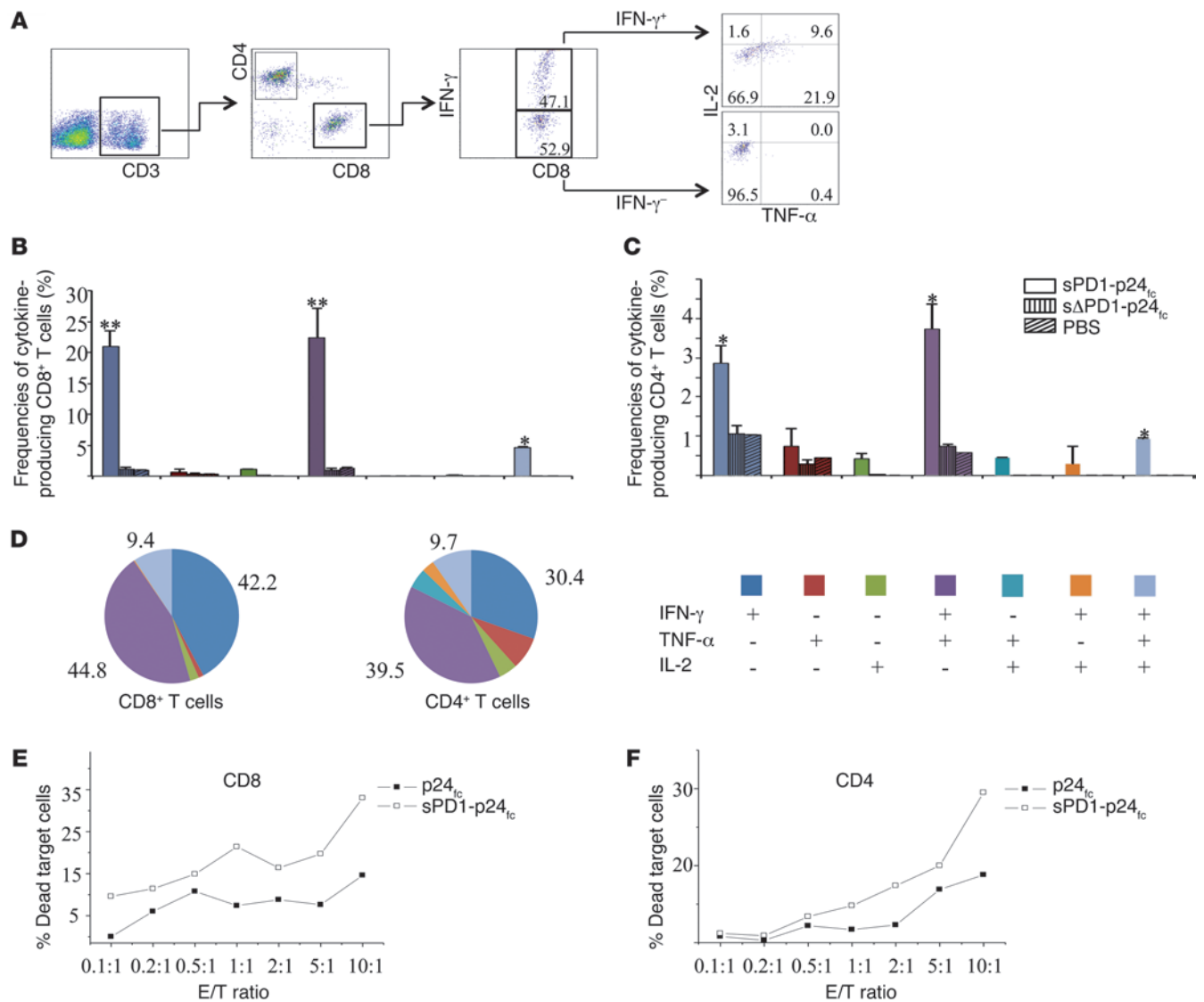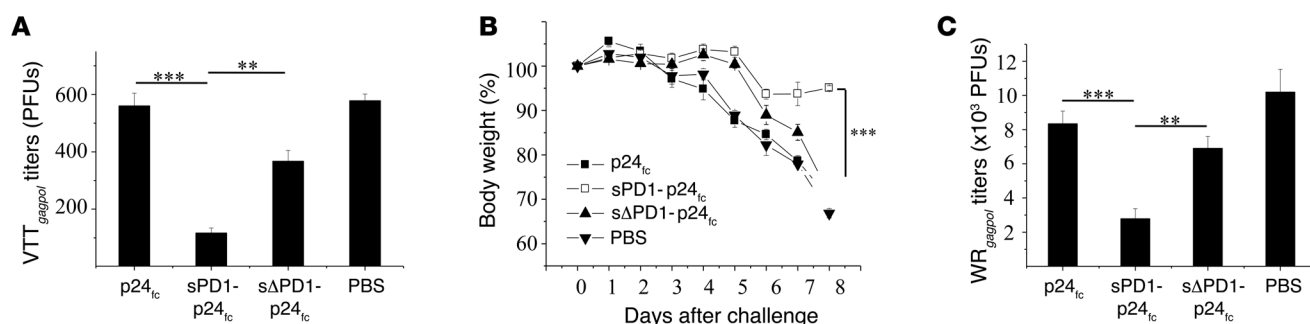
Figure 5
Polyfunctionality and cytotoxicity effects of sPD1-p24$_{fc}$–induced T cells. BALB/c mice were immunized by i.m./EP with 3 injections of 100 μg sPD1-p24$_{fc}$ and sΔPD1-p24$_{fc}$. Splenocytes were collected and analyzed by flow cytometry following intracellular staining using antibodies against IFN-γ, TNF-α, and IL-2. (**A**) Gating strategy for flow cytometric scatter plots to analyze the frequency of CD8$^+$ or CD4$^+$ T cells positive for IFN-γ, TNF-α, and/or IL-2. (**B**) Column graphs depicting subpopulations of single-, double-, or triple-positive CD8$^+$ or (**C**) CD4$^+$ T cells releasing the cytokines IFN-γ, TNF-α, and IL-2 induced by DNA vaccination of sPD1-p24$_{fc}$ and sΔPD1-p24$_{fc}$ (and PBS control). (**D**) Pie chart analysis representing subpopulations of total cytokine-secreting CD8$^+$ or CD4$^+$ T cells positive for combinations of IFN-γ, TNF-α, and IL-2. Columns and pie regions represent the mean values of 2 independent experiments with 3 mice per group, with error bars representing the SEM. (**E**) Purified CD8$^+$ or (**F**) CD4$^+$ T cells from sPD1-p24$_{fc}$– and p24$_{fc}$-immunized mice were stimulated by p24 peptide pools plus anti-CD28 overnight before cytotoxicity assay with an AB1-HIV-1-GAG cell line as the target. Line graphs show the percentages of dead cells as a result of cell-mediated killing, with the baseline of natural target cell death percentage subtracted. *$P < 0.05$; **$P < 0.01$.

of IgG1 responses (Supplemental Figure 2). Thus, in our experimental conditions, the adjuvant effect of sPD1$_{fc}$ was minimal, while the fusion protein was necessary for effective DC targeting. Finally, the EP/no-Fc group induced levels of T cell (IFN-γ$^+$CD8$^+$ or IFN-γ$^+$CD4$^+$) and antibody responses comparable to those in mice vaccinated with rabbit Fc-containing counterparts in group 1 (Supplemental Figure 2), indicating that the Fc portion of the DNA fusion vaccine did not affect immunogenicity against HIV-1 GAG p24. Overall, these findings indicate that the fusion DNA

construct of sPD1-p24$_{fc}$, combined with EP, is essential and is the best strategy for eliciting greatly enhanced CD8$^+$ T cell and antibody responses. To further study the in vivo DC-targeting effect of sPD1-based DNA vaccination, we constructed sPD1-OVA$_{fc}$ and sΔPD1-OVA$_{fc}$ plasmids by replacing HIV-1 p24 antigen. We introduced CFSE-labeled OT-I cells into C57BL/6 mice 24 hours before vaccination via sPD1-OVA$_{fc}$/EP, sΔPD1-OVA$_{fc}$/EP, and sPD1-p24$_{fc}$/EP, respectively. Five days later, OT-I cells in draining lymph nodes were analyzed by CFSE signals using flow cytometry.

Figure 6

sPD1-based DNA vaccination–induced antigen-specific immunity confers protection against virulent viral challenge. (**A**) Mice previously immunized with 20-μg DNA vaccines were challenged with 4×10^7 PFUs VTT$_{gagpol}$ three weeks after immunization to examine immune protection. Virus titers in the lungs of immunized mice were evaluated by examining plaque formation on Vero cell monolayers 3 days after challenge. Mice immunized with 100-μg DNA vaccines were challenged with 2×10^6 PFUs WR$_{gagpol}$ three weeks after immunization and weighed daily for 8 days. (**B**) Body weight percentage loss from day 0. (**C**) Mice were sacrificed on day 8 and virus titers in the lungs were evaluated by examining plaque formation on Vero cell monolayers. Data represent the SEM of 2 independent experiments with 5 mice per group. **P < 0.01; ***P < 0.001.

The results showed that, indeed, OVA-specific CD8+ T cells had greatly proliferated in mice injected with sPD1-OVA$_{fc}$ compared with sΔPD1-OVA$_{fc}$ and nonspecific sPD1-p24$_{fc}$ controls (Supplemental Figure 3), confirming enhanced in vivo DC targeting for antigen presentation.

sPD1-p24$_{fc}$/EP is more effective than anti–DEC205-p24/EP at enhancing CD8+ T cell immunity. Anti-DEC205 antibody has been previously used to develop DC-targeting vaccines (15, 16). Here, we investigated the immunogenicity of 2 DC-targeting DNA vaccines, sPD1-p24$_{fc}$ and single-chain anti–DEC205-p41 (16), compared with non–DC-targeting controls, p24$_{fc}$, p41 and PBS, in parallel experiments following the standard immunization schedule with a 100-μg dosage delivered via i.m./EP (Figure 2A). ELISPOT assay showed that sPD1-p24$_{fc}$/EP and anti–DEC205-p41/EP elicited considerably higher levels of p24-specific CD8+ and CD4+ T cells than did p24$_{fc}$/EP and p41/EP (Figure 7, A and B). Against the single GAG A-I epitope, sPD1-p24$_{fc}$/EP induced a significant 3-fold greater level of CD8+ T ELISPOTs than anti–DEC205-p41/EP (*P* < 0.05). Moreover, consistent with previous experiments, sPD1-p24$_{fc}$/EP induced close to 20% of the tetramer-positive CD8+ T cell populations, while anti–DEC205-p41/EP induced about half of that percentage, though this was higher than in the controls (Figure 7C). Analysis of the p24-specific antibody titers revealed that sPD1-p24$_{fc}$/EP and anti–DEC205-p41/EP were similar for both IgG1 and IgG2a (Figure 7D). In addition, we examined polyfunctional CD8+ and CD4+ T cell subsets after p24 peptide pool stimulation. As shown in Figure 7E, statistically significantly higher frequencies of CD8+ T cells were evident with sPD1-p24$_{fc}$/EP than with anti–DEC205-p41/EP across 4 subpopulations, including IFN-γ+ alone (2.5-fold higher), IFN-γ+/TNF-α+ (4-fold higher), IFN-γ+/IL-2+ (5-fold higher), and IFN-γ+/TNF-α+/IL-2+ (5-fold higher) (all *P* < 0.05). CD4+ T cells also displayed the same trend, but *P* values did not reach statistical significance (Figure 7F). These data demonstrate the overall superiority of sPD1-based DNA vaccine in enhancing antigen-specific CD8+ T cells compared with anti-DEC205–mediated DC-targeting DNA vaccine.

sPD1-p24$_{fc}$/EP vaccination uniquely enhances IL-12–producing DCs in vivo. To further investigate the underlying mechanism of sPD1-p24$_{fc}$/EP vaccination compared with anti–DEC205-p41/EP, we sought to determine the effects of the former on DCs in terms

of antigen uptake, maturation and activation, and Th1 cytokine production — all of which may influence adaptive immunity (43, 44). Although PD-L1 expressed in B cells and macrophages may lead to a broader cell range than DEC205 for exogenous antigen presentation, only DCs are capable of activating or cross-priming naive CD8+ T cells (45, 46). For proof-of-concept, we purified splenic CD11c+ DCs from mice and treated them with purified proteins sPD1-p24$_{fc}$, p24$_{fc}$, or anti–DEC205-p24 (28). We found that both anti–DEC205-p24 and sPD1-p24$_{fc}$ protein bound to splenic CD11c+ DCs in vitro at similar and much higher levels than did p24$_{fc}$ protein (Supplemental Figure 4A), indicating proper binding with their respective receptors. Moreover, the detection of p24 antigen intracellularly after sPD1-p24$_{fc}$ (~6%) or anti–DEC205-p24 (~12%) binding (Supplemental Figure 4B) suggests that antigen uptake had taken place. We then examined these findings in vivo. Groups of BALB/c mice were immunized with 100 μg of sPD1-p24$_{fc}$, anti–DEC205-p41 (16), or p24$_{fc}$ DNA via i.m./EP, and were sacrificed at 8, 16, and 24 hours to examine the level of p24 antigen uptake as well as the levels of costimulatory molecules and Th1 cytokines in CD11c+ DCs in draining lymph nodes. We consistently found that mice vaccinated with sPD1-p24$_{fc}$/EP and anti–DEC205-p41/EP displayed higher intracellular p24 signals compared with DCs from p24$_{fc}$ or PBS control mice at 8 hours (Supplemental Figure 5A). These results indicate that there was no significant difference between the 2 DC-targeting strategies in terms of antigen binding and uptake by DCs both in vitro and in vivo. Compared with the p24$_{fc}$/EP control, however, only sPD1-p24$_{fc}$/EP elicited statistically significantly higher expression of CD40 and MHC class II molecules on CD11c+ DCs at 16 hours in the draining lymph nodes (Figure 8, A and B; *P* < 0.05). We also found a relatively higher level of CD80 (Supplemental Figure 5B), but not CD86 (data not shown), expression on CD11c+ DCs at 24 hours despite the lack of statistical significance, suggesting direct effects on DC activation after sPD1-p24$_{fc}$/EP. For comparison, no changes were found in PD-L1/L2 expression on DCs or PD1 expression on T cells in vivo (data not shown). Furthermore, we examined the production of Th1 cytokines IL-12 and IFN-γ by CD11c+ DCs (47). Interestingly, the frequency of IL-12–producing CD11c+ DCs was found to be significantly higher in the sPD1-p24$_{fc}$/EP group than in the anti–DEC205-p41/EP or
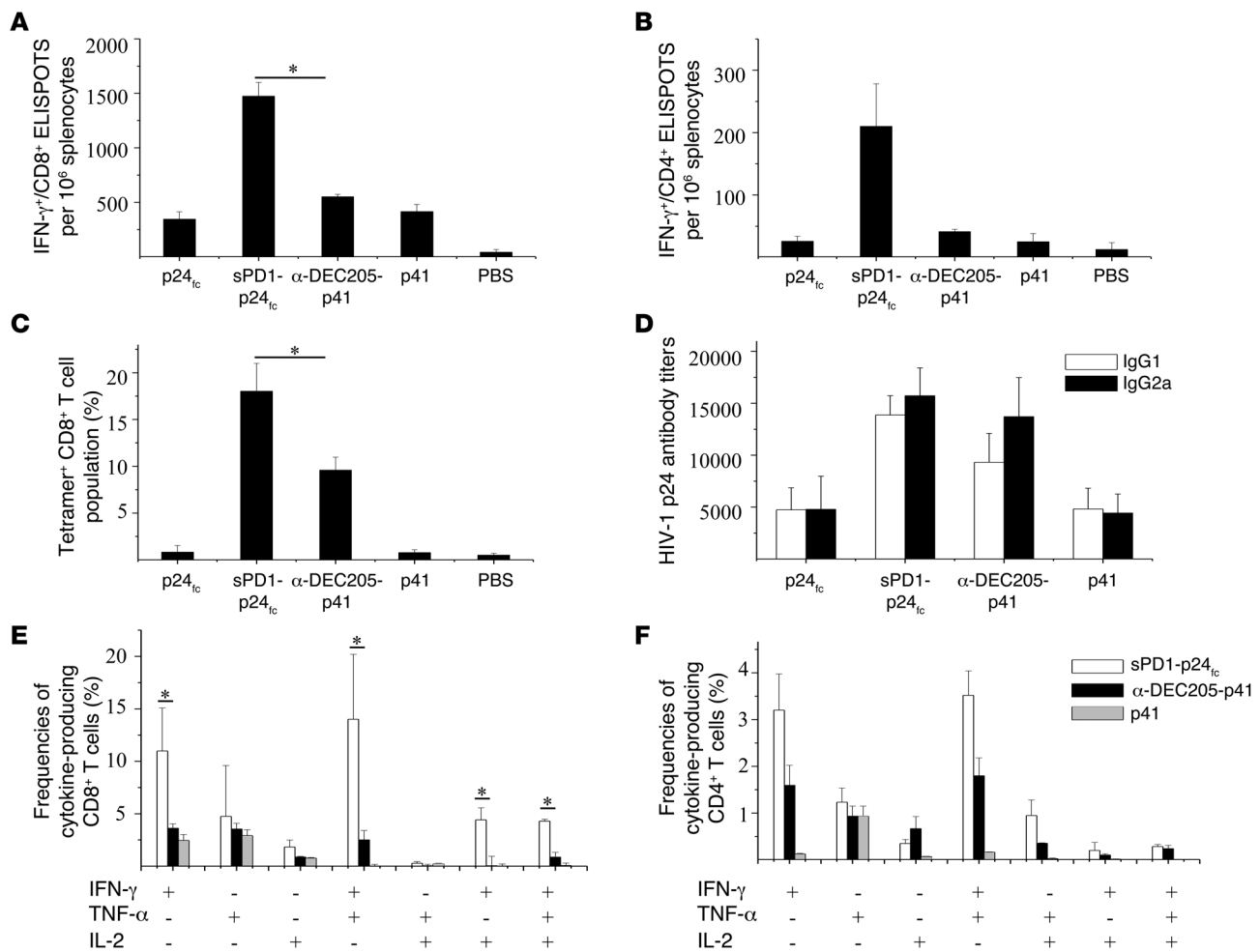
Figure 7
DNA immunization of mice with sPD1-based vaccines elicits stronger antigen-specific CD8+ T cell responses compared with DEC205-based vaccines. BALB/c mice were administered 2 different DC-targeting DNA vaccines of sPD1-p24$_{fc}$ and psc-DEC205-p41 at a dose of 100 μg delivered via i.m./EP. p24$_{fc}$, (psc-)Cont-p41, and PBS were used as controls. (**A**) IFN-γ–producing CD8+ and (**B**) CD4+ cells were measured by ELISPOT assay in splenocytes stimulated with the specific epitopes GAG A-I and GAG 26, respectively. (**C**) HIV-1 p24–specific H2-K^d-AMQMLKDTI-PE tetramer staining of CD8+ T cell populations is represented as a column graph of immunization. (**D**) Specific IgG1 and IgG2a antibodies against HIV-1 GAG p24 were detected in sera by ELISA. Intracellular staining performed on both CD4+ and CD8+ T cell populations in splenocytes is shown in column graphs depicting subpopulations of single-, double-, and triple-positive (**E**) CD8+ or (**F**) CD4+ T cells releasing the cytokines IFN-γ, TNF-α, and IL-2 induced by DNA vaccination. Data show the SEM with 5 mice per group. *$P < 0.05$.

p24$_{fc}$/EP groups (Figure 8C; $P < 0.05$). On the other hand, the frequency of IFN-γ–producing DCs was found to be similar between the sPD1-p24$_{fc}$/EP and anti–DEC205-p41/EP groups (Figure 8D), but higher than that of the p24$_{fc}$/EP group. Thus, these results suggest that although both DC-targeting strategies could activate DC production of IFN-γ, sPD1-p24$_{fc}$/EP displayed a unique advantage in the activation of IL-12–producing DCs in vivo, which is important for the activation of CD8+ T cell immunity (45, 48).

sPD1-p24$_{fc}$, but not anti–DEC205-p24, engages the antigen cross-presentation pathway in DCs. Since sPD1-p24$_{fc}$/EP or anti–DEC205-p41/EP resulted in comparable p24 binding and uptake (Supplemental Figure 4 and Supplemental Figure 5A), but the former generated higher CD8+ T cell response in vivo, we speculated that the underlying antigen presentation pathway for CD4+ and CD8+ T cell activation is distinct (49). It has been documented that cross-presenta-

tion of exogenous antigen by DCs can drive the subsequent CD8+ T cell response independent of CD4+ T cell help (49, 50). After exogenous antigen uptake by DCs, the antigen is localized to early endosomes (Rab5+), then diverted to the Rab14+ compartment through MHC class I cross-presentation for CD8+ T cell activation (46) or late endosomal (Rab9+ or Lamp1+) routing to the lysosomal compartment that is apparently required for adequate processing and MHC class II presentation and subsequent CD4+ T cell activation (49, 51, 52). Thus, we performed colocalization experiments using p24 antigen and biomarkers of endosomal compartments in splenic CD11c+ DCs. We used sPD1-p24, anti–DEC205-p24, and p24 proteins (without the Fc tag) to treat DCs for 15 minutes, 30 minutes, 1 hour, and 2 hours, respectively. Confocal microscopic analysis showed that both sPD1-p24 and anti–DEC205-p24 were colocalized with early Rab5+ endosomes, as well as with late Rab7+
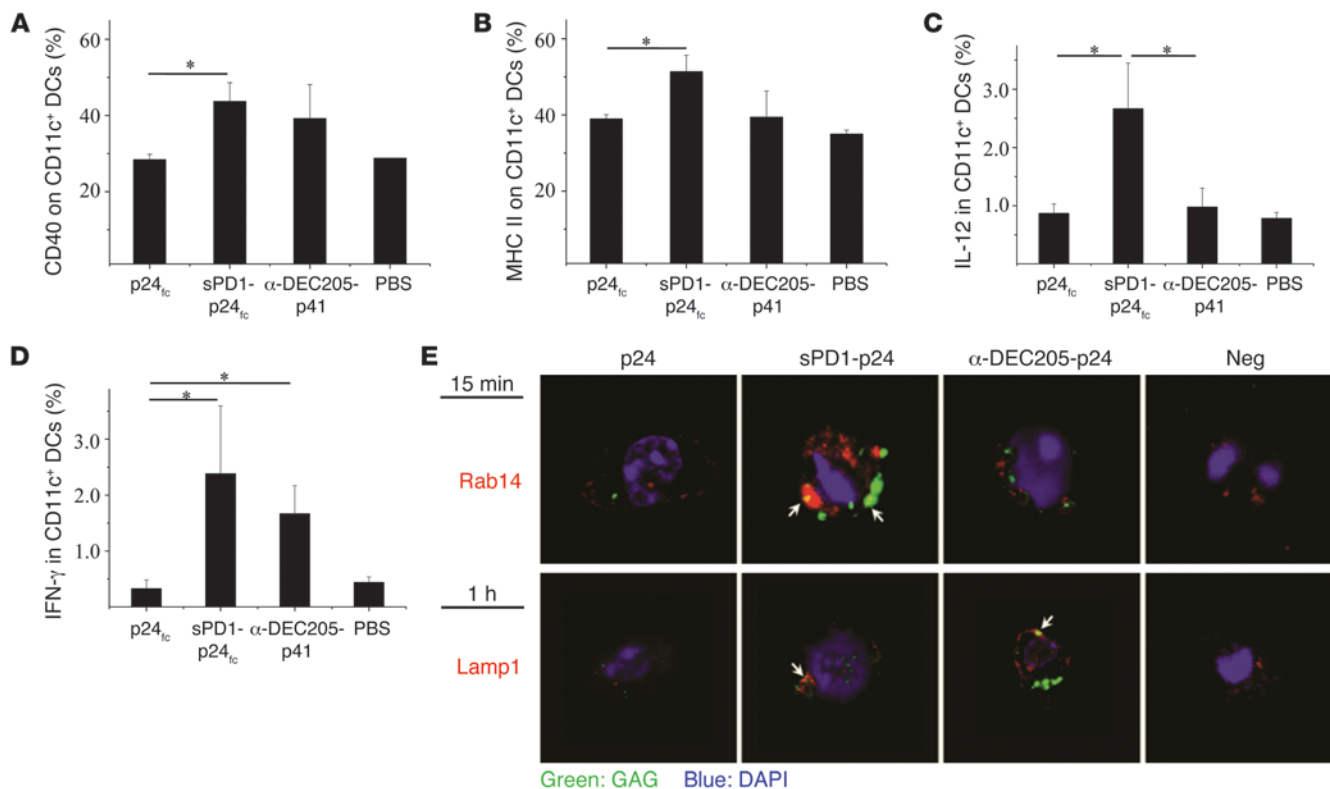
Figure 8

sPD1-based vaccine functions by activating DCs and engaging in cross-presentation. Mice were immunized with sPD1-p24$_{fc}$, anti–DEC205-p41, and p24$_{fc}$ DNA vaccines, or PBS placebo, at a 100-μg dose administered by i.m./EP. Column graphs show (**A**) surface expression of CD40 and (**B**) MHC II, as well as intracellular staining of (**C**) IL-12 and (**D**) IFN-γ in draining lymph node CD11c$^+$ DCs 16 hours after immunization. Data show the SEM with 5 mice per group. *$P < 0.05$. (**E**) Purified splenic CD11c$^+$ DCs were treated with the proteins sPD1-p24, anti–DEC205-p24, or p24 for 15 minutes and 1 hour. Formaldehyde-fixed DCs were immunostained for HIV-1 GAG, Rab 14, and Lamp1. Nuclei were counterstained with DAPI. Images are overlays of the 3 signals (green: GAGp24; red: endosomal marker; blue: DAPI). (**F**) Schematic representation of the underlying mechanisms of sPD1-based vaccine. Following DC targeting of sPD1-p24$_{fc}$ (red arrows), antigen uptake into Rab5 endosomes was diverted to: (a) Rab14 endosomal compartment for subsequent MHC I cross-presentation; or (b) Rab7, Rab9, and Lamp1 endosomes, leading to MHC II presentation. Antigen presentation and activation of respective T cells are likely accompanied by increased costimulatory CD40 expression and production of Th1 cytokines IFN-γ and IL-12. By comparison, DC targeting of anti–DEC205-p24 (green arrows) was only routed to Lamp1 endosomes with induced IFN-γ production. Nontargeting p24 was only found in Rab7 endosomes (dotted blue arrow). The red cross symbol represents the HIV-1 antigen p24.

and Rab9$^+$ endosomes, and were subsequently found with Lamp1 endosomes from 30 minutes to 1 hour onward when compared with the p24 controls (Figure 8D and Supplemental Figure 6). Importantly, by 15 minutes, sPD1-p24, but not anti–DEC205-p24, was found colocalized with Rab14 (Figure 8E and Supplemental Figure 6; the quantification of colocalization is shown in Supplemental Table 1). These data demonstrate that while both DC-targeting strategies engage MHC class II (Lamp1) endosomes for the induction of CD4$^+$ T cell responses, sPD1-p24 uniquely used the cross-presenting MHC class I (Rab14) endosomal compartments that likely underlie the enhanced CD8$^+$ T cell response following vaccination (Figure 8F).

Discussion

In this study, we demonstrate that the sPD1-p24$_{fc}$/EP DNA vaccination elicits remarkably enhanced cellular and humoral immune responses against HIV-1 GAG antigen. To the best of our knowledge, this is the first DNA vaccine strategy in BALB/c mice to use PD1 for the induction of strong HIV-1 GAG-specific CD8$^+$ T cell immunity with broad reactivity, long-term memory, polyfunctionality, cytotoxicity, and protective function, which is unique compared with existing DNA vaccines. The markedly enhanced CD8$^+$ T cell response is mainly due to more efficient antigen targeting to DCs, as well as to the subsequent activation and Th1 cytokine production of DCs in the draining lymph nodes of immunized mice compared with that achieved by non–DC-targeting vaccines. In addition to these findings, sPD1-based vaccination displays unique advantages when compared with anti–DEC205–based DC targeting in its capacity to induce a higher frequency of IL-12–producing DCs and to engage the antigen cross-presentation pathway in DCs for antigen-specific CD8$^+$ T cell potentiation. Since DNA vaccination is safe and has no preexisting immunity issues (53), sPD1-based vaccine may offer a new and effective way to induce a high frequency of durable antigen-specific CD8$^+$ T cell immunity, which has implications for the prevention and treatment not only of HIV-1/AIDS but also of other infectious diseases and even cancer.

A high frequency of anti-GAG CD8$^+$ T cell immunity is considered a critical characteristic of an effective T cell–based vaccine designed to suppress and contain SIV/HIV infections and facilitate the elimination of the latent viral reservoir after viral reactivation (9, 40, 54, 55). Here, sPD1-p24$_{fc}$/EP DNA vaccination not only elicited high frequencies of IFN-γ$^+$ spot–forming and tetramer-positive HIV-1–specific CD8$^+$ T cells, but improved their polyfunctionality and cytotoxicity and conferred substantial protection against mucosal challenge in mice with 2 types of vaccinia GAG viruses. As measured by ELISPOT assay for the specific CD8$^+$ T cell epitope GAG A-I, sPD1-p24$_{fc}$/EP elicited approximately 900 SFUs per 10^6 splenocytes at the 20-μg DNA dose, and a further rise to over 1,600 SFUs per 10^6 splenocytes at the 100-μg DNA dose (Figure 2B and Figure 3A). Compared with our previous DNA or viral vector–based vaccine candidates, 1 mg ADVAX (a codon-optimized HIV-1 DNA vaccine) administered i.m. only induced approximately 250 SFUs per 10^6 splenocytes (31), whereas the modified vaccinia Ankara–vectored (MVA-vectored) HIV-1 vaccine ADMVA induced approximately 200 SFUs per 10^6 splenocytes against the GAG A-I epitope in BALB/c mice after 2 i.m. vaccinations at a dose of 10^6 TCID$_{50}$ (32). Even for adjuvant-assisted DNA vaccination in BALB/c mice against the same GAG A-I epitope, i.m. coadministration of IL-15 and HIV-1 GAG

DNA elicited approximately 200–610 SFUs per 10^6 splenocytes at a dose of 50 to 100 μg DNA (56, 57). In addition, the 22% CD8$^+$ GAG A-I tetramer–positive T cell response elicited with the 100-μg dose of sPD1-p24$_{fc}$/EP (Figure 4) was comparable to that obtained with rAd5-GAG vaccines in BALB/c mice immunized 3 times at a high dose of 10^{10} virus particles, and to that observed in BALB/c mice immunized by a heterologous prime-boost protocol with 2 live vectors (*L. monocytogenes* and Ad5) or by a DC-directed (via DC-SIGN) lentiviral system encoding HIV-1 GAG protein (39, 58). Furthermore, we show that up to 47.1% of total splenic CD8$^+$ T cells were p24 specific and were releasing IFN-γ$^+$ after GAG peptide pool stimulation (Figure 5A). And within the cytokine-producing CD8$^+$ T cell population, the proportional distribution of polyfunctional T subsets followed the order of IFN-γ$^+$/TNF-α$^+$ being greater than IFN-γ$^+$, which in turn was greater than IFN-γ$^+$/TNF-α$^+$/IL-2$^+$ (Figure 5D). These types of greatly enhanced polyfunctional anti-GAG CD8$^+$ T cell immunity were neither found with the 2 control vaccines in our parallel experiments, nor reported by the existing DNA vaccine strategies described above (56, 57, 59). Importantly, consistent with enhanced cytotoxic CD8$^+$ and CD4$^+$ T cell activity (Figure 5, E and F), challenge studies using 2 types of vaccinia GAG viruses have demonstrated the significantly improved vaccine efficacy offered by sPD1-p24$_{fc}$/EP (Figure 6; $P < 0.01$). These findings suggest the potential for the development of an effective PD1-based DNA vaccine against HIV/AIDS in the future (9, 40).

Compared with non–DC-targeting vaccines, one of the key underlying mechanisms of sPD1-p24$_{fc}$/EP vaccination depends on the functionality of sPD1 for more effective antigen targeting to DCs and subsequent enhanced DC activation in vivo. In this study, besides p24$_{fc}$, we included sΔPD1-p24$_{fc}$ as a non–DC-targeting control. sΔPD1-p24$_{fc}$ differs from sPD1-p24$_{fc}$ by 2 essential amino acids in the functional IgV domain of sPD1 (35, 36, 60), which renders the protein unable to interact with PD1 ligands expressed on either transfected cells (Figure 1C) or DCs (data not shown). Since there were substantial differences between sPD1-p24fc/EP and sΔPD1-p24$_{fc}$/EP in eliciting GAG-specific adaptive immunity (Figures 2–5), the intact sPD1 IgV domain is apparently essential to the functionality of the sPD1-based antigen in DC targeting. Our preliminary data showing a higher level of proliferating OVA-specific OT-I cells after sPD1-OVA$_{fc}$/EP vaccination provide further evidence for the role of sPD1-based DC targeting in CD8$^+$ T cell potentiation in vivo (Supplemental Figure 3). Furthermore, we demonstrate that the sPD1-p24$_{fc}$ fusion construct for DC targeting is critical because codelivery of sPD1$_{fc}$ and p24$_{fc}$ in trans by EP at the same or different anatomic sites did not achieve significantly enhanced CD8$^+$ T cell response compared with sPD1-p24$_{fc}$/EP (Supplemental Figure 2). This finding also suggests that the level of sPD1$_{fc}$ expression after EP vaccination likely does not achieve a strong adjuvant effect by blocking the PD1/PD-L signaling pathway to produce the same level of CD8$^+$ T cell expression as sPD1-p24$_{fc}$. In addition, unlike the non–DC-targeting p24$_{fc}$/EP control, sPD1-p24$_{fc}$/EP resulted in consistently higher levels of CD40, CD80, and MHC class II expression, as well as Th1 cytokine IL-12 and IFN-γ production in DCs, suggesting an increased DC activation in draining lymph nodes that is critical for the potentiation of CD8$^+$ T cell responses (Figure 8, A–D, Supplemental Figure 5B) (44, 45).

Various DC-targeting strategies that include DNA vaccines delivered by EP to strengthen HIV-1 GAG-specific immunity have been explored previously by others, but with limited suc-

cess in amplifying CD8+ T cell immune responses (14–17). To further determine the underlying mechanism of an sPD1-based vaccine, we directly compared it with the conventional anti–DEC205–based DC-targeting approach (16, 28). By performing sPD1-p24$_{fc}$/EP and anti–DEC205-p41/EP vaccination in mice, we found that although both strategies elicited statistically insignificant levels of CD4+ T cell and antibody responses (Figure 7, B and D), sPD1-p24$_{fc}$/EP induced significantly greater numbers of antigen-specific CD8+ T cells by ELISPOT (Figure 7A; $P < 0.05$), tetramer staining (Figure 7C; $P < 0.05$), and intracellular assays (Figure 7E; $P < 0.05$). We then investigated the role of costimulatory molecules, Th1-polarizing cytokine production, and antigen presentation/cross-presentation pathways in DCs, all of which may enhance antigen-specific CD8+ T cell immunity as previously described (61). When we examined the DCs in draining lymph nodes after vaccination, we found that sPD1-p24$_{fc}$/EP and anti–DEC205-p41/EP achieved comparable levels of antigen uptake (Supplemental Figure 5A), costimulatory molecule expression (Figure 8A), and a similar frequency of IFN-γ–producing DCs (Figure 8D). In contrast, a noticeably higher frequency of IL-12–producing DCs was only detected with sPD1-p24$_{fc}$/EP vaccination, suggesting that an IL-12–mediated mechanism underlies the increase in CD8+ T cell response (47). This finding is in line with the notion that DC-produced IL-12 is the primary cytokine enhancing the frequency of IFN-γ–producing antigen–specific CD8+ T cells (Figure 5, A–D) (45). It is also in line with our data showing that p24 antigen delivered by sPD1-p24 is routed to Rab14 endosomes for MHC class I presentation to CD8+ T cells (46), as well as to late Lamp1 endosomes for MHC class II presentation to CD4+ T cells, which is used by both DC-targeting strategies to induce similar CD4+ T cell and antibody responses (Figure 7B, Figure 8, E and F) (49, 51, 52). These findings are novel, we believe, and suggest that antigen targeting to DCs via different surface receptors may activate distinct intercellular pathways for IL-12 production and antigen cross-presentation. Future studies, however, should be conducted to reveal the endocytic function following sPD1 binding to PD-L1/L2, the induction of IL-12 expression, and to determine whether a difference in antigen uptake and processing occurs in other more defined DC subsets (46, 62).

Methods

Construction of sPD1-based vaccine and controls. We constructed 3 DNA vaccines: sPD1-p24$_{fc}$, sΔPD1-p24$_{fc}$, and p24$_{fc}$ on a background of pVAX1 (Figure 1A). The coding sequence for the extracellular domain of murine PD1 (sPD1) was obtained by nested PCR from mouse cDNA (mPD1F-B: 5′-CGCGGATCCGCG ATGTGGGTCCGGCAGGTA-3′; mPD1B-E: 5′-CCGGAATTCCGGTTGAAACCG GCCTTCTGG-3′), and the HIV-1 p24 fragment was amplified from a primary isolate HIV-1$_{02HNsq4}$ of a Chinese patient without codon optimization. To increase the flexibility of the fusion protein, a linker GGGGSGGGG (nt sequence: GGTGGT-GGTTCAGGAGGAGGA) was applied between the sPD1 and HIV1 p24 gene. A mutant form of sPD1 (sΔPD1) was also cloned following the same strategy as used with wild-type PD1. sΔPD1 does not react with PD1 ligands due to an in-frame deletion of 2 essential amino acids (position 89-90) in the IgV domain. Plasmid expressing HIV-1 p24 alone served as a control. All plasmids contained a rabbit Fc tag to facilitate protein purification and characterization. Plasmids without a rabbit Fc tag, or sPD1 without p24, were generated by restriction enzyme digestion and re-ligation, and were verified by sequencing. DNA transfection into (HEK-)293T cells was per-

formed using polyethylenimine (PEI), and protein expression was detected by Western blot using both anti-rabbit Fc and anti-HIV GAG antibodies. Recombinant proteins were purified from the transfected cell supernatants by affinity chromatography using Protein G Sepharose (Invitrogen), and protein concentration was measured using a Micro BCA Protein Assay Kit (Thermo Scientific).

Binding characteristics of sPD1 fusion proteins. 293T cells (10^6 cells) transiently expressing PD-L1 and PD-L2 were incubated with 2 μg of purified sPD1-p24$_{fc}$, sΔPD1-p24$_{fc}$, or p24$_{fc}$ fusion protein. Goat anti-rabbit IgG (HL)-FITC (Invitrogen) was used to capture the positive signals. Transfected 293T cells stained by FITC-rat anti-mouse PD-L1 or PD-L2 antibodies (eBioscience) and FITC-rat IgG1 isotype served as positive and negative controls, respectively. Data were acquired on a FACSCalibur instrument (BD Biosciences) and analyzed using CellQuest software (BD Biosciences).

Mouse immunization. All animal experiments were approved by the Committee on the Use of Live Animals in Teaching and Research at the Laboratory Animal Unit of The University of Hong Kong. Five- to 8-week-old female BALB/c mice and C57BL/6 mice were bred under standard pathogen-free conditions in the Laboratory Animal Unit of The University of Hong Kong. Mice were housed in cages under standard conditions with regulated temperature and humidity, fed with pelted food and tap water, and cared for according to the criteria outlined in the Guide for the Care and Use of Laboratory Animals. OT-I and OT-II mice were provided by Kang Liu and were kept in the Rockefeller University laboratory (New York, New York, USA). The immunization procedure was similar to our previous protocols. Mice received 3 DNA immunizations by i.m. injection with or without EP given every 3 weeks at a dose of 20 μg or 100 μg per mouse. Two weeks after every immunization, blood samples were taken for sera antibody testing. Two weeks after the final immunization, the mice were sacrificed, and sera and splenocytes were collected for immune response analysis (Figure 2A).

ELISA. Specific antibody responses were assessed by ELISA as previously described (42). Briefly, high-affinity, protein-binding ELISA plates (BD Biosciences) were coated with HIV-1 p24 protein (Abcam). Serial-diluted sera were then added and antibodies detected with HRP-labeled anti-mouse IgG1 or IgG2a (or IgG2c for C57BL/6 mice sera) antibody (Sigma-Aldrich). Relative antibody titers were expressed as the reciprocal highest dilution of samples producing at least a 2-fold greater optical density readout than that of the control serum sample at the same dilution.

Evaluation of HIV-1 Gag p24-specific T cell responses. IFN-γ–producing T cells were evaluated by an ELISPOT assay (Millipore) as previously described (32). Ten micrograms per milliliter of HIV-1 p24 peptide or peptide pools (at a final concentration of 2 μg/ml for each peptide, donated by the NIH, catalog no. 8117) were used to stimulate splenocytes in vitro. Peptide pools consisting of 59-member GAG p24 libraries (each peptide contained 15aa with 10aa overlap) were divided into 3 pools of 19 to 20 peptides spanning amino acids 1–87 (pool 1), 77–167 (pool 2), and 157–231 (pool 3). Peptide GAG A-I (AMQMLKDTI) is specific to CD8+ T cells, whereas peptide GAG 26 (TSNPPIPVGDIYKRWIILGL) is specific to CD4+ T cells. Cells stimulated with 500 ng/ml phorbol 12-mystrate 13-acetate (PMA; Sigma-Aldrich) plus 1 μg/ml calcium ionocycin or left in media only served as positive and negative controls, respectively. Cells were incubated at 37°C, 5% CO$_2$, and 100% humidity for 20 hours. Spots were identified by an immunospot reader and image analyzer (Thermo Scientific). For intracellular cytokine staining (ICS), splenocytes were stimulated with an HIV-1 p24 peptide pool (2 μg/ml for each peptide) in the presence of costimulatory anti-CD28 antibody (2 μg/ml, eBioscience) for 20 to 24 hours at 37°C. Brefeldin A (10 μg/ml; Sigma-Aldrich) was added for the last 5 hours to accumulate intracellular cytokines. Cells were washed and incubated with 2.4G2 mAb for 15 minutes at 4°C to block Fcγ. After

research article

surface staining with anti-mouse CD3-APC/Cy7, CD4-PE/Cy5, and CD8-PerCP/Cy5.5 antibodies (eBioscience), cells were permeabilized in 100 μl of Fixation/Permeabilization solution (BD Biosciences) for 20 minutes at 4°C, washed with Perm/Wash buffer (BD Biosciences), and then stained intracellularly with anti–IFN-γ-PE, anti–IL-2-PE-Cy7, and anti–TNF-α-FITC (eBioscience). Tetramer-positive CD8+ T cell populations were evaluated using PE-conjugated MHC class I tetramer H2d-Kd-AMQMLKDTI (Beckman Coulter).

T cell proliferation assay. Splenocytes isolated from BALB/c mice 30 weeks after the final immunization were labeled with CFSE (10^7 cells/ml in PBS, 1 μM, 10 minutes at 37°C water bath; Invitrogen). Labeled cells were stimulated with bone marrow–derived DCs (BM-DCs) at a ratio of 10:1 in the presence of HIV-1 GAG p24 peptide pools (2 μg/ml), and anti-CD28 (2 μg/ml) or anti-CD3 (0.1 μg/ml) antibodies were used as positive controls. BM-DCs from BALB/c mice were obtained from bone marrow extracts and cultured for 7 days in the presence of murine GM-CSF (10 U/ml; Sigma-Aldrich) and IL-4 (10 U/ml; Sigma-Aldrich), then enriched using a Dynabeads Mouse CD11c+ DC Enrichment Kit (Invitrogen). Five days after coculture, cells were collected and stained with CD3-APC/Cy7, CD4-PE/Cy5, CD8-PerCP/Cy5.5 antibodies. Flow cytometric data were acquired and analyzed on a FACSAria III flow cytometer (BD Biosciences).

Cytotoxicity assay. AB1 cells were purchased from the European Collection of Cell Cultures. Cells were cultured in RPMI1640 supplemented with 10% FBS, L-glutamine, and antibiotics. The cell line was maintained in vitro at 37°C in a humidified atmosphere containing 5% CO_2. Based on the original pBABE-puro vector, we generated the transfer vector pBABE-HIVgag/Luc for the construction of the AB1-HIVgag-luc cell line, which encodes a fusion form of the full-length HIV *gag* gene with firefly luciferase. Since the original LTR promoter on the vectors is considered a weak promoter, we inserted a CMV promoter obtained from the pVAX1 vector and inserted it upstream of the fusion gene to drive a higher level of transcription and protein expression. Retrovirus was packaged by cotransfection of the pCL packaging vector and transfer plasmid (pBABE-HIVgag/Luc) into 293T cells. Retrovirus-containing supernatants were collected and used to infect AB1 cells followed by puromycin selection. Single clones were selected by limiting dilution of the drug-resistant cells in 96-well plates. Following single clone cultures, HIV GAG expression was confirmed and validated by flow cytometry. Then we used the LIVE/DEAD Viability/Cytotoxicity Kit (Invitrogen) to assess the cytotoxic effects of purified CD4+ and CD8+ T cells isolated from vaccinated mice (Dynabeads CD4 Negative Isolation Kit and Dynabeads CD8 Negative Isolation Kit; Invitrogen). Purified T cells and target AB1-HIV-1-GAG cells were cocultured for 2 hours at 37°C then analyzed for the percentage of dead target cells in total AB1-HIV-1-GAG cell populations on an FACSCalibur instrument (BD Biosciences) using CellQuest software (BD Biosciences).

Vaccinia viral challenge. Immunized mice were challenged intranasally by 4×10^7 PFUs of a modified vaccinia Tian Tan strain or 2×10^6 PFUs of the vaccinia Western Reserve (WR) strain, which expresses HIV *gag* and *pol* genes. The pathogenic vaccinia WR strain was purchased from ATCC (ATCC VR-1354) and propagated in Vero cells. The virus was modified to express HIV-1 *gag* and *pol* genes in place of the hemagglutinin gene. Animal body weight was monitored daily. Groups of animals were also sacrificed 3 days or 8 days after challenge by VTT*gagpol* or WR*gagpol,* respectively, to measure viral titers in their lungs. Lung homogenates were prepared by physical disruption and by passing cells through cell strainers, and virus titers in the lungs were determined by a plaque-forming assay on monolayer Vero cells and monitored for cytopathic effect over time.

Comparison of anti-DEC205- and sPD1-based vaccines. The single chain of anti–mouse DEC205 fused with HIV-1 p41 psc-DEC-p41 (antigen p41 consists of p24 and p17) and control plasmid psc-Cont-p41 were provided by

Godwin Nchinda. Protein expression of these plasmids from transfected 293T cells was detected at similar levels by Western blot analysis (data not shown). The DNAs psc-DEC-p41, psc-Cont-p41, sPD1-p24fc, and p24fc were used to immunized mice via i.m./EP at a dose of 100 μg. PBS served as a control. The immunization procedure and immune response analysis were the same as described above.

Effects of sPD1-based vaccine on DCs. Splenocytes isolated from naive BALB/c mice were enriched using a Dynabeads Mouse CD11c+ DC Enrichment Kit (Invitrogen). The expression plasmids of encoded anti-mouse DEC205 fused to HIV GAG p24 was provided by Christine Trumpfheller. CD11c+ splenic DCs (1×10^6) were treated with purified sPD1-p24fc or anti–DEC205-p24, p24fc proteins for 20 minutes at room temperature. Goat anti-rabbit IgG (HL)-FITC (Invitrogen) was used to capture the positive signals. FITC-rat anti-mouse PD-L1 or PD-L2 antibodies (eBioscience) were used to confirm the expression of PD1 ligands on the surface of DCs. Goat anti-rabbit IgG (HL)-FITC stained with DCs cultured in medium only served as a negative control. FITC-rat anti-mouse PD-L1 or PD-L2 antibodies (eBioscience) were used to confirm the expression of PD1 ligands on the surface of DCs. Goat anti-rabbit IgG (HL)-FITC stained with DCs cultured in medium only served as a negative control. For antigen uptake analysis, 1×10^6 splenic CD11c+ DCs were cultured with 2 μg of purified sPD1-p24fc or sΔPD1-p24fc, anti-DEC205-p24 antibody, and p24fc proteins at 4°C for 1 hour. PBS served as a negative control. Cells were collected and permeabilized in 100 μl of Fixation/Permeabilization solution (BD Biosciences) for 20 minutes at 4°C, washed with Perm/Wash buffer (BD Biosciences), and then stained intracellularly with goat anti-rabbit IgG (HL)-FITC. Data were acquired on an FACSCalibur instrument (BD Biosciences) and analyzed using CellQuest software (BD Biosciences).

For in vivo antigen targeting analysis, DNA vaccines of sPD1-p24fc or sΔPD1-p24fc, anti–DEC205-p41, and p24fc were administered i.m. with EP to BALB/c mice at a 100-μg dose. PBS served as a negative control. Mice were sacrificed at 4, 8, 16, 24, and 72 hours after injection. Draining lymph nodes were extracted and single cells were isolated. Cells were stained with surface antibodies: anti-CD11c-APC/Cy7; anti-MHC II-PE; anti–CD80-APC; anti–CD86-PerCP/Cy5.5; anti–CD40-PE/Cy5; anti–PD-1-PE/Cy7; anti–PD-L1-PE; anti–PD-L2-FITC; and anti–CD3-Pacific Blue (eBioscience). These stained cells were permeabilized in 100 μl of Fixation/Permeabilization solution (BD Biosciences) for 20 minutes at 4°C, washed with Perm/Wash buffer (BD Biosciences), and then stained intracellularly with FITC-conjugated mouse anti–HIV-1 p24 antibody (KC57 FITC; Beckman Coulter), FITC-conjugated anti-mouse IL-12 (eBioscience), and PE-conjugated anti-mouse IFN-γ (eBioscience). Flow cytometric data were acquired and analyzed on a FACSAria III flow cytometer (BD Biosciences).

To confirm in vivo antigen presentation, we constructed sPD1-OVAfc and sPD1-OVAfc by replacing HIV-1 p24 antigen with ovalbumin (OVA). C57BL/6 mice were immunized with sPD1-OVAfc, and controls with sΔPD1-OVAfc and sPD1-p24fc delivered by i.m./EP at a dose of 100 μg DNA. The next day, 2×10^6 CFSE-labeled OT-I or OT-II T cells were adoptively transferred into B6 mice by tail vein injection. Five days after immunization, draining lymph nodes were harvested and the extent of CFSE dilution determined among OT-I or OT-II T cells by flow cytometry.

Immunofluorescence. Splenic DCs were enriched from total splenocytes using a Dynabeads Mouse CD11c+ DC Enrichment Kit (Invitrogen), seeded on a 96-well black plate (ibidi) overnight, and treated with p24, sPD1-p24, or anti–DEC205-p41 proteins at 37°C for 15 minutes, 30 minutes, 1 hour, and 2 hours. After treatment, cells were briefly centrifuged and fixed with 2% paraformaldehyde for 40 minutes at room temperature as previously described (49). Next, permeabilization using

blocking buffer PBS with 5% FBS, 3% BSA, and 0.5% Triton X-100 was performed for 20 minutes at 4°C before incubation with primary antibodies against Rab5, Rab7, Rab9, Rab14, Lamp1 (Sigma-Aldrich), and anti–HIV-1 GAG monoclonal antibody for 12 hours at 4°C in a staining buffer of PBS with 3% BSA and 0.1% Triton X-100. Secondary antibodies Alexa Fluor 488 donkey anti-mouse and Alexa Fluor 555 donkey anti-rabbit IgG (Invitrogen) were used for fluorescence staining at room temperature for 1 hour, followed by mounting using SlowFade Gold antifade reagent with DAPI. Signals were acquired using a Carl Zeiss LSM 700 microscope and images were analyzed using ZEN software. ImageJ software (http://imagej.nih.gov/ij/, 1997–2012) (63) with a JACoP plug-in was used to calculate various colocalization coefficients: Pearson's correlation, overlap coefficient, and Mander's coefficient, as reported in Supplemental Table 1.

Statistics. All statistical analyses were performed using the 2-tailed Student's *t* test. *P* values less than 0.05 were considered statistically significant. Data are presented as the mean values ± SEM of at least 3 independent experiments unless otherwise indicated.

Study approval. Handling, experimental procedures including injections, blood collection, virus challenge, and sacrificing were approved and performed according to the University of Hong Kong Committee on the Use of Live Animals in Teaching and Research (CULATR 1881-09 and 1922-09).

Address correspondence to: Zhiwei Chen, AIDS Institute and Department of Microbiology, Li Ka Shing Faculty of Medicine, The University of Hong Kong, L5-45, 21 Sassoon Road, Pokfulam, Hong Kong SAR, China. Phone: 852.2819.9831; Fax: 852.2817.7805; E-mail: zchenai@hku.hk.

1. Moorthy A, et al. Induction therapy with protease-inhibitors modifies the effect of nevirapine resistance on virologic response to nevirapine-based HAART in children. *Clin Infect Dis*. 2011;52(4):514–521.
2. Luo M, et al. Prevalence of drug-resistant HIV-1 in rural areas of Hubei province in the People's Republic of China. *J Acquir Immune Defic Syndr*. 2009;50(1):1–8.
3. Killian MS, Levy JA. HIV/AIDS: 30 years of progress and future challenges. *Eur J Immunol*. 2011;41(12):3401–3411.
4. Li Q, et al. Visualizing antigen-specific and infected cells in situ predicts outcomes in early viral infection. *Science*. 2009;323(5922):1726–1729.
5. Makedonas G, Betts MR. Living in a house of cards: re-evaluating CD8+ T-cell immune correlates against HIV. *Immunol Rev*. 2011;239(1):109–124.
6. Schmitz JE, et al. Control of viremia in simian immunodeficiency virus infection by CD8+ lymphocytes. *Science*. 1999;283(5403):857–860.
7. Virgin HW, Walker BD. Immunology and the elusive AIDS vaccine. *Nature*. 2010;464(7286):224–231.
8. Hansen SG, et al. Profound early control of highly pathogenic SIV by an effector memory T-cell vaccine. *Nature*. 2011;473(7348):523–527.
9. Liu J, et al. Immune control of an SIV challenge by a T-cell-based vaccine in rhesus monkeys. *Nature*. 2009;457(7225):87–91.
10. Barouch DH, et al. Immunogenicity of recombinant adenovirus serotype 35 vaccine in the presence of pre-existing anti-Ad5 immunity. *J Immunol*. 2004;172(10):6290–6297.
11. Vasan S, et al. Phase 1 safety and immunogenicity evaluation of ADVAX, a multigenic, DNA-based clade C/B' HIV-1 candidate vaccine. *PLoS One*. 2010;5(1):e8617.
12. Gurunathan S, Klinman DM, Seder RA. DNA vaccines: immunology, application, and optimization*. *Annu Rev Immunol*. 2000;18:927–974.
13. Vasan S, et al. In vivo electroporation enhances the immunogenicity of an HIV-1 DNA vaccine candidate in healthy volunteers. *PLoS One*. 2011;6(5):e19252.
14. Deliyannis G, Boyle JS, Brady JL, Brown LE, Lew AM. A fusion DNA vaccine that targets antigen-presenting cells increases protection from viral challenge. *Proc Natl Acad Sci U S A*. 2000;97(12):6676–6680.
15. Idoyaga J, et al. Comparable T helper 1 (Th1) and CD8 T-cell immunity by targeting HIV gag p24 to CD8 dendritic cells within antibodies to Langerin, DEC205, and Clec9A. *Proc Natl Acad Sci U S A*. 2011;108(6):2384–2389.
16. Nchinda G, et al. The efficacy of DNA vaccination is enhanced in mice by targeting the encoded protein to dendritic cells. *J Clin Invest*. 2008;118(4):1427–1436.
17. Zhang W, Chen Z, Huang Y, Song Y, Ho DD. CTLA4-mediated APC-targeting enhanced the humoral and cellular immune responses of an SIV DNA vaccine in mice. In: *10th Conference on Retroviruses and Opportunistic Infections*. Boston, Massachusetts, USA: Foundation for Retrovirology and Human Health; 2003. Abstract 397.
18. You Z, Huang X, Hester J, Toh HC, Chen SY. Targeting dendritic cells to enhance DNA vaccine potency. *Cancer Res*. 2001;61(9):3704–3711.
19. Latchman Y, et al. PD-L2 is a second ligand for PD-1 and inhibits T cell activation. *Nat Immunol*. 2001;2(3):261–268.
20. Freeman GJ, et al. Engagement of the PD-1 immunoinhibitory receptor by a novel B7 family member leads to negative regulation of lymphocyte activation. *J Exp Med*. 2000;192(7):1027–1034.
21. Kasprowicz V, et al. High level of PD-1 expression on hepatitis C virus (HCV)-specific CD8+ and CD4+ T cells during acute HCV infection, irrespective of clinical outcome. *J Virol*. 2008;82(6):3154–3160.
22. Day CL, et al. PD-1 expression on HIV-specific T cells is associated with T-cell exhaustion and disease progression. *Nature*. 2006;443(7109):350–354.
23. Trautmann L, et al. Upregulation of PD-1 expression on HIV-specific CD8+ T cells leads to reversible immune dysfunction. *Nat Med*. 2006;12(10):1198–1202.
24. Flies DB, Sandler BJ, Sznol M, Chen L. Blockade of the B7-H1/PD-1 pathway for cancer immunotherapy. *Yale J Biol Med*. 2011;84(4):409–421.
25. He L, Zhang G, He Y, Zhu H, Zhang H, Feng Z. Blockade of B7-H1 with sPD-1 improves immunity against murine hepatocarcinoma. *Anticancer Res*. 2005;25(5):3309–3313.
26. Sharpe AH, Wherry EJ, Ahmed R, Freeman GJ. The function of programmed cell death 1 and its ligands in regulating autoimmunity and infection. *Nat Immunol*. 2007;8(3):239–245.
27. Velu V, et al. Enhancing SIV-specific immunity in vivo by PD-1 blockade. *Nature*. 2009;458(7235):206–210.
28. Trumpfheller C, et al. Intensified and protective CD4+ T cell immunity in mice with anti-dendritic cell HIV gag fusion antibody vaccine. *J Exp Med*. 2006;203(3):607–617.
29. Kiepiela P, et al. CD8+ T-cell responses to different HIV proteins have discordant associations with viral load. *Nat Med*. 2007;13(1):46–53.
30. Altfeld M, Goulder PJ. THE STEP study provides a hint that vaccine induction of the right CD8+ T cell responses can facilitate immune control of HIV. *J Infect Dis*. 2011;203(6):753–755.
31. Huang Y, et al. Design, construction, and characterization of a dual-promoter multigenic DNA vaccine directed against an HIV-1 subtype C/B' recombinant. *J Acquir Immune Defic Syndr*. 2008;47(4):403–411.
32. Chen Z, Huang Y, Zhao X, Ba L, Zhang W, Ho DD. Design, construction, and characterization of a multigenic modified vaccinia Ankara candidate vaccine against human immunodeficiency virus type 1 subtype C/B'. *J Acquir Immune Defic Syndr*. 2008;47(4):412–421.
33. Fitzgerald DW, et al. An Ad5-vectored HIV-1 vaccine elicits cell-mediated immunity but does not affect disease progression in HIV-1-infected male subjects: results from a randomized placebo-controlled trial (the Step study). *J Infect Dis*. 2011;203(6):765–772.
34. Rerks-Ngarm S, et al. Vaccination with ALVAC and AIDSVAX to prevent HIV-1 infection in Thailand. *New Engl J Med*. 2009;361(23):2209–2220.
35. Lazar-Molnar E, Yan Q, Cao E, Ramagopal U, Nathenson SG, Almo SC. Crystal structure of the complex between programmed death-1 (PD-1) and its ligand PD-L2. *Proc Natl Acad Sci U S A*. 2008;105(30):10483–10488.
36. Lin DY, et al. The PD-1/PD-L1 complex resembles the antigen-binding Fv domains of antibodies and T cell receptors. *Proc Natl Acad Sci U S A*. 2008;105(8):3011–3016.
37. Liu L, et al. Natural mutations in the receptor binding domain of spike glycoprotein determine the reactivity of cross-neutralization between palm civet coronavirus and severe acute respiratory syndrome coronavirus. *J Virol*. 2007;81(9):4694–4700.
38. Aihara H, Miyazaki J. Gene transfer into muscle by electroporation in vivo. *Nat Biotechnol*. 1998;16(9):867–870.

research article

39. Dai B, Yang L, Yang H, Hu B, Baltimore D, Wang P. HIV-1 Gag-specific immunity induced by a lentivector-based vaccine directed to dendritic cells. *Proc Natl Acad Sci U S A*. 2009;106(48):20382–20387.

40. Ferrari G, et al. Relationship between functional profile of HIV-1 specific CD8 T cells and epitope variability with the selection of escape mutants in acute HIV-1 infection. *PLoS Pathog*. 2011;7(2):e1001273.

41. Davis MR, Manning LS, Whitaker D, Garlepp MJ, Robinson BW. Establishment of a murine model of malignant mesothelioma. *Int J Cancer*. 1992;52(6):881–886.

42. Fang Q, et al. Host range, growth property, and virulence of the smallpox vaccine: vaccinia virus Tian Tan strain. *Virology*. 2005;335(2):242–251.

43. Moser M, Murphy KM. Dendritic cell regulation of TH1-TH2 development. *Nat Immunol*. 2000;1(3):199–205.

44. Trinchieri G. Interleukin-12 and the regulation of innate resistance and adaptive immunity. *Nat Rev Immunol*. 2003;3(2):133–146.

45. Henry CJ, Ornelles DA, Mitchell LM, Brzoza-Lewis KL, Hiltbold EM. IL-12 produced by dendritic cells augments CD8+ T cell activation through the production of the chemokines CCL1 and CCL17. *J Immunol*. 2008;181(12):8576–8584.

46. Weimershaus M, Maschalidi S, Sepulveda F, Manoury B, van Endert P, Saveanu L. Conventional dendritic cells require IRAP-Rab14 endosomes for efficient cross-presentation. *J Immunol*. 2012;188(4):1840–1846.

47. Joffre O, Nolte MA, Sporri R, Reis e Sousa C. Inflammatory signals in dendritic cell activation and the induction of adaptive immunity. *Immunol Rev*. 2009;227(1):234–247.

48. Asakura Y, et al. Th1-biased immune responses induced by DNA-based immunizations are mediated via action on professional antigen-presenting cells to up-regulate IL-12 production. *Clin Exp Immunol*. 2000;119(1):130–139.

49. De Luca A, et al. CD4(+) T cell vaccination overcomes defective cross-presentation of fungal antigens in a mouse model of chronic granulomatous disease. *J Clin Invest*. 2012;122(5):1816–1831.

50. Thacker RI, Janssen EM. Cross-presentation of cell-associated antigens by mouse splenic dendritic cell populations. *Front Immunol*. 2012;3:41.

51. Chikhlikar P, et al. DNA encoding an HIV-1 Gag/human lysosome-associated membrane protein-1 chimera elicits a broad cellular and humoral immune response in Rhesus macaques. *PLoS One*. 2006;1:e135.

52. Bonini C, Lee SP, Riddell SR, Greenberg PD. Targeting antigen in mature dendritic cells for simultaneous stimulation of CD4+ and CD8+ T cells. *J Immunol*. 2001;166(8):5250–5257.

53. Voltan R, Robert-Guroff M. Live recombinant vectors for AIDS vaccine development. *Curr Mol Med*. 2003;3(3):273–284.

54. Koup RA, Douek DC. Vaccine design for CD8 T lymphocyte responses. *Cold Spring Harb Perspect Med*. 2011;1(1):a007252.

55. Turnbull EL, et al. HIV-1 epitope-specific CD8+ T cell responses strongly associated with delayed disease progression cross-recognize epitope variants efficiently. *J Immunol*. 2006;176(10):6130–6146.

56. Li W, Li S, Hu Y, Tang B, Cui L, He W. Efficient augmentation of a long-lasting immune responses in HIV-1 gag DNA vaccination by IL-15 plasmid boosting. *Vaccine*. 2008;26(26):3282–3290.

57. Kutzler MA, et al. Coimmunization with an optimized IL-15 plasmid results in enhanced function and longevity of CD8 T cells that are partially independent of CD4 T cell help. *J Immunol*. 2005;175(1):112–123.

58. Li Z, Zhang M, Zhou C, Zhao X, Iijima N, Frankel FR. Novel vaccination protocol with two live mucosal vectors elicits strong cell-mediated immunity in the vagina and protects against vaginal virus challenge. *J Immunol*. 2008;180(4):2504–2513.

59. Widera G, et al. Increased DNA vaccine delivery and immunogenicity by electroporation in vivo. *J Immunol*. 2000;164(9):4635–4640.

60. Wang S, Bajorath J, Flies DB, Dong H, Honjo T, Chen L. Molecular modeling and functional mapping of B7-H1 and B7-DC uncouple costimulatory function from PD-1 interaction. *J Exp Med*. 2003;197(9):1083–1091.

61. Kapsenberg ML. Dendritic-cell control of pathogen-driven T-cell polarization. *Nat Rev Immunol*. 2003;3(12):984–993.

62. Saveanu L, et al. IRAP identifies an endosomal compartment required for MHC class I cross-presentation. *Science*. 2009;325(5937):213–217.

63. Schneider CA, Rasband WS, Eliceiri KW. NIH Image to ImageJ: 25 years of image analysis. *Nat Methods*. 2012;9(7):671–675.